ICCK

Journal of Nonlinear Dynamics and Applications
http://dx.doi.org/10.62762/JNDA.2025.975574

RESEARCH ARTICLE

Predefined-Time Synchronization Control of Fractional Cohen-Grossberg Neural Networks with Non-Identical Fractional Orders under Time-Varying Delays

Chaouki Aouiti[1] **and El Abed Assali**[1,2,*]

[1] Department of Mathematics, Faculty of Sciences of Bizerte, University of Carthage, Bizerte 7021, Tunisia
[2] Higher School of Engineering of Medjez el Bab (ESIM), University of Jendouba, Medjez el Bab, Tunisia

Abstract

In this paper, we study the problem of predefined-time synchronization for distinct-order fractional delayed Cohen-Grossberg neural networks. Fractional-order models are known for their ability to capture memory effects and complex dynamics more accurately than classical integer-order systems. In particular, allowing distinct-order in the drive and response systems provides additional flexibility in modeling. To achieve synchronization, we propose two control strategies that provide sufficient conditions for predefined-time synchronization of the addressed model. These strategies are based on the construction of an appropriate Lyapunov function and the use of fractional calculus properties. Finally, two numerical examples are provided to verify the effectiveness of the proposed methods.

Keywords: fractional-order, neural networks, predefined-time, synchronization, control.

Submitted: 08 October 2025
Accepted: 12 December 2025
Published: 16 December 2025

Vol. 1, **No.** 2, 2025.
10.62762/JNDA.2025.975574

***Corresponding author:**
✉ El Abed Assali
elabed.assali@fsb.rnu.tn

1 Introduction

Over the past few years, neural networks (NNs) have attracted significant attention due to their wide range of applications in fields such as associative memory, signal and image processing, and pattern recognition [1–3]. Notable examples include Hopfield NNs [4], bidirectional associative memory NNs [5], and Cohen–Grossberg NNs (CohGNNs) [6, 7], the latter of which, introduced by Cohen and Grossberg in 1983 [8], have received considerable attention from researchers and have been extensively studied. Moreover, it is important to acknowledge that time delays are common in real-world systems and can significantly influence the stability of NNs. This issue has been examined by Li et al. [9], who investigated how such delays affect network behavior. As a result, studying how time delay effects can be incorporated into CohGNNs presents an interesting and valuable research direction.

As an important subject within NNs, control [10–12] and chaos synchronization [13] have drawn significant interest because of their applications in biological systems [14], secure communication [2], and other fields. Nonetheless, much of the prior research has primarily addressed asymptotic synchronization. That is, synchronization usually occurs only in the long term. However, in practical control [15], especially in

Citation
Aouiti, C., & Assali, E. A. (2025). Predefined-Time Synchronization Control of Fractional Cohen-Grossberg Neural Networks with Non-Identical Fractional Orders under Time-Varying Delays. *Journal of Nonlinear Dynamics and Applications*, 1(2), 99–111.

engineering, it is often necessary for the network to synchronize within a finite period. Finite-time control also brings advantages like enhanced robustness and better resistance to interference [16].

Furthermore, studies on finite-time synchronization [17–19] aim to achieve synchronization in the shortest possible time. However, the actual time needed to stabilize the system is generally influenced by its initial state. In practice, it is often impossible to know or measure all initial conditions of a system. To address this challenge, Polyakov [20] introduced the concept of fixed-time stability, where the convergence time is guaranteed to be uniform and independent of the initial conditions of the system. By removing the dependency on initial conditions, fixed-time control has gained considerable attention and has been widely applied to the study of CohGNNs [16, 21–23]. For example, the authors in [16] studied the problem of finite-time and fixed-time synchronization for delayed CohGNNs with memristor connection weights. The authors in [21] explored a fixed-time synchronization of memristive CohGNNs with impulsive effects. Kong et al. [22] studied the fixed-time synchronization of CohGNNs with mixed time delays and discontinuous neuron activations. Tan et al. [23] studied the fixed-time synchronization in multilayer networks CohGNNs with delay via adaptive quantitative control. It is worth noting that in certain cases, adjusting the system parameters is not enough to reduce the settling time below a desired constant. As a result, predefined-time (P_fT) stability has been developed in recent years. Unlike fixed-time stability, where the settling time is fixed but independent of system parameters, P_fT stability offers a direct link between the settling time and system parameters, allowing it to be set in advance according to practical needs. In [24], the authors studied the P_fT synchronization Control of Memristive integer-order CohGNNs with time-varying delay.

On the other hand, fractional calculus, which generalizes classical calculus by extending derivatives and integrals to non-integer (arbitrary) orders, has a history that spans more than 300 years [25, 26]. Although fractional calculus has been studied for centuries, its practical applications in physics and engineering have gained significant attention only in recent years [27]. Compared to traditional integer-order systems, fractional-order systems offer enhanced modeling capabilities, particularly for processes that exhibit memory and hereditary properties. This makes them especially suitable for accurately representing real-world phenomena such as viscoelastic materials, mechanical systems, and signal processing tasks. Given these advantages, it becomes important to explore fractional-order Cohen–Grossberg neural networks (FRCohGNNs), as incorporating fractional dynamics can improve their ability to model complex systems with greater flexibility and precision [30].

Based on the available literature, the synchronization results discussed in previous studies for FRCohGNNs with the same orders [27–29]. In [27], the authors studied the synchronization and stability of FRCohGNNs with parameter mismatches and external perturbations. In [28], the authors investigated finite-time synchronization of delayed FRCohGNNs, developing new fractional-order inequalities and feedback control strategies to improve the estimation of settling times. In [29], the authors studied the finite-time stability and synchronization of memristor-based FRCohGNNs using set-valued maps and Filippov differential inclusions. The study in [27–29] focused on synchronizing two FRCohGNNs configured in a drive–response structure and sharing the same fractional order. Assuming identical orders in drive-response systems may fail to capture the complexities encountered in real-world scenarios. Achieving synchronization between systems with differing orders is crucial for designing more flexible and selective models for information processing [34].

Note that synchronization in non-identical fractional-order chaotic systems allows for a more flexible response mechanism, as it accounts for differences in system dynamics. This flexibility makes it particularly relevant for modeling real-world systems. In this context, we study P_fT synchronization of FRCohGNNs with distinct fractional orders, which poses additional challenges compared to the identical-order case in [30]. In particular, the challenges posed by non-identical fractional orders include how to properly define the error system when the drive and response dynamics evolve under different derivative orders, and how to construct a controller that guarantees predefined-time convergence despite the mismatch in fractional orders. These issues do not appear in identical-order synchronization studies and require specific analytical techniques. Moreover, to address these challenges, we have constructed two different controllers that offer advantages in terms of structural simplicity and broader applicability, making them suitable for a wider class of fractional-order neural network models

with distinct-order.
Building on the above discussions, this paper focuses on solving the P_fT problem of distinct-order FRCohGNNs using two types of control strategies. The main contributions of this work are outlined below.

1. A novel P_fT synchronization is developed for FRCohGNNs, where the drive and response systems have different fractional orders, reflecting more realistic and flexible modeling scenarios.
2. Two control methods are proposed:
   - a fractional-order controller, tailored to handle systems with fractional dynamics;
   - a controller without fractional derivatives, offering a simpler structure while still ensuring synchronization within a predefined time.
3. Numerical simulations are presented to validate the effectiveness and efficiency of the proposed controllers, demonstrating their ability to synchronize FRCohGNNs within the predefined time.

The rest of this paper is organized as follows. Section 2 introduces some fundamental definitions and lemmas, along with the distinct-order FRCohGNNs model. In Section 3, we develop two control methods to achieve P_fT synchronization. Section 4 presents a numerical example that validates the effectiveness of the proposed theorem. Finally, Section 5 concludes the paper and outlines potential directions for future research.

2 Preliminaries and useful results

In this section, we introduce the concept of fractional order, describe the structure of the FRCohGNNs model, and outline the main assumptions used in our analysis.

Definition 1 *The Gamma function, denoted by $\Gamma(s)$, is defined for any real number $s > 0$ by the improper integral:*

$$\Gamma(s) = \int_0^{+\infty} t^{s-1}e^{-t}\,du.$$

Definition 2 *If $\hbar(t) \in C([0,+\infty),\mathbb{R})$ is an integrable function, the Caputo type fractional order integral is defined as follows:*

$${}_{t_0}^{C}I_t^{\alpha}\hbar(t) = {}_{t_0}^{C}D_t^{-\alpha}\hbar(t) = \frac{1}{\Gamma(\alpha)}\int_{t_0}^{t}(t-s)^{\alpha-1}\hbar(s)\mathrm{d}s$$

where $t \geq t_0 \geq 0, \alpha > 0$.

Definition 3 *Let $\hbar(t) \in C([0,+\infty),\mathbb{R})$ be an integrable function. The Caputo fractional derivative of order α is defined as follows:*

$${}_{t_0}^{C}D_t^{\alpha}\hbar(t) = \frac{1}{\Gamma(n-\alpha)}\int_{t_0}^{t}(t-s)^{n-\alpha-1}\hbar^{(n)}(s)\mathrm{d}s$$

where $t \geq t_0 \geq 0$, $\alpha \in (n-1,n), n \in \mathbb{Z}^+$.

Proposition 1 [35] *If $\hbar(t)$ is a function in $C^n([t_0,+\infty),\mathbb{R})$, and $0 \leq \beta \leq \lambda$ are constants, then the Caputo derivative satisfies the following property:*

$${}_{t_0}^{C}D_{tt_0}^{\beta C}D_t^{-\lambda}\hbar(t) = {}_{t_0}^{C}D_t^{\beta-\lambda}\hbar(t),$$

$${}_{t_0}^{C}D_{tt_0}^{\beta C}D_t^{-\beta}\hbar(t) = \hbar(t),$$

$${}_{t_0}^{C}D_{tt_0}^{-\gamma C}D_t^{\gamma}\hbar(t) = \hbar(t) - \hbar(t_0),$$

where $\gamma \in (0,1)$.

Remark 1 *For the sake of simplicity, we refer to*

$${}_{t_0}^{C}D_t^{\gamma}\hbar(t) = D^{\gamma}\hbar(t),$$

where t_0 denotes the initial time. For the purposes of this paper, we set $t_0 = 0$

In this paper, we consider the FRCohGNNs described below, which includes time-varying delays:

$$\begin{aligned} D^{\gamma}x_i(t) &= -\alpha_i(x_i(t))\Big(\beta_i(x_i(t)) - \sum_{j=1}^{n}c_{ij}g_j(x_j(t)) \\ &\quad - \sum_{j=1}^{n}d_{ij}h_j(x_j(t-\sigma(t))) - I_i\Big), \end{aligned} \tag{1}$$

where $i = 1,2,\cdots,n$; $\gamma \in (0,1)$; I_i represents the external input to neuron i; $x_i(t)$ stands for the state variable associated with the i^{th} neuron; $\alpha_i(x_i(t))$ represents the amplification function; $\beta_i(x_i(t))$ is a function with appropriate regularity; c_{ij} and d_{ij} denote the synaptic connection strengths between neurons; g_j and h_j represent the activation functions; $\sigma(t)$ refers to the delay that varies over time caused by the finite speed of axonal signal transmission, and satisfies $0 \leq \sigma(t) \leq \sigma$.
The initial condition of system (1) is given by

$$x_i(\theta) = \phi_i(\theta), \quad \theta \in [-\sigma,0],$$

where $\phi_i \in C([-\sigma,0],\mathbb{R})$.

Equation (1) represents the drive system of the examined drive–response systems, while the response system is given by:

$$\begin{aligned} D^{\delta}y_i(t) &= -\alpha_i\left(y_i(t)\right)\Big(\beta_i\left(y_i(t)\right) - \sum_{j=1}^{n} c_{ij}g_j\left(y_j(t)\right) \\ &- \sum_{j=1}^{n} d_{ij}h_j\left(y_j(t-\sigma(t))\right) - I_i\Big) \\ &+ U_{1i,2i}(t), \end{aligned} \tag{2}$$

with initial conditions

$$y_i(\theta) = \varphi_i(\theta), \quad \theta \in [-\sigma, 0],$$

where $U_{1i,2i}(t)$ is the control input that needs to be designed.
Let $\epsilon_i(t) = y_i(t) - x_i(t)$ denote the error system for the drive and response systems (1)–(2). Then, the error dynamics between the drive system (1) and the response system (2) are defined as follows:

$$\begin{cases} D^{\delta}\epsilon_i(t) = D^{\delta}y_i(t) - D^{\delta}x_i(t) \\ = D^{\delta}y_i(t) - D^{\gamma}x_i(t) - D^{\delta}x_i(t) + D^{\gamma}x_i(t) \\ = -\alpha_i\left(y_i(t)\right)\Big(\beta_i\left(y_i(t)\right) - \sum_{j=1}^{n} c_{ij}g_j\left(y_j(t)\right) \\ - \sum_{j=1}^{n} d_{ij}h_j\left(y_j(t-\sigma(t))\right) - I_i\Big) + U_{1i,2i}(t) \\ +\alpha_i\left(x_i(t)\right)\Big(\beta_i\left(x_i(t)\right) - \sum_{j=1}^{n} c_{ij}g_j\left(x_j(t)\right) \\ - \sum_{j=1}^{n} d_{ij}h_j\left(x_j(t-\sigma(t))\right) - I_i\Big) \\ -D^{\delta}x_i(t) + D^{\gamma}x_i(t), \end{cases} \tag{3}$$

with initial conditions

$$y_i(\theta) - x_i(\theta) = \varphi_i(\theta) - \phi_i(\theta), \quad \theta \in [-\sigma, 0],$$

The following hypotheses are introduced to establish the main results

(H1) For all $j = 1, 2, \cdots, n$, the activation functions $g_j(x)$ and $h_j(x)$ are bounded and Lipschitz continuous. Specifically, there exist positive constants G_j, H_j, L_j^g, L_j^h such that for all $x, y \in \mathbb{R}$,

$$\begin{aligned} |g_j(x)| &\le G_j, \\ |h_j(x)| &\le H_j, \\ |g_j(y) - g_j(x)| &\le L_j^g|y - x|, \\ |h_j(y) - h_j(x)| &\le L_j^h|y - x|. \end{aligned}$$

(H2) The amplification function $\alpha_i(x_i(t))$ is continuous and bounded for all $i = 1, 2, \cdots, n$, satisfying:

$$\underline{\alpha_i} \le \alpha_i(x_i(t)) \le \overline{\alpha_i},$$

where $\underline{\alpha_i}$ and $\overline{\alpha_i}$ are positive constants. Moreover, there exists a constant $\lambda_i > 0$ such that:

$$|\alpha_i(y(t)) - \alpha_i(x(t))| \le \lambda_i|y(t) - x(t)|.$$

(H3) The product of the amplification function $\alpha_i(x(t))$ and $\beta_i(x(t))$ satisfies the inequality:

$$|\alpha_i(y(t))\beta_i(y(t)) - \alpha_i(x(t))\beta_i(x(t))| \le \varpi_i|y(t) - x(t)|,$$

for all $x, y \in \mathbb{R}$, $i = 1, 2, \cdots, n$, where $\varpi_i > 0$ is a constant.

Definition 4 *The drive FRCohGNNs (1) and the response FRCohGNNs (2) are said to achieve finite-time synchronization if, for any solutions $x(t) = (x_1(t), \cdots, x_n(t))^T$ and $y(t) = (y_1(t), \cdots, y_n(t))^T$ with initial conditions ϕ_i and φ_i, there exists a finite constant $0 \le T_{finite-time} < +\infty$, which may depend on these initial conditions, such that:*

$$\lim_{t \to T_{finite-time}} \|y(t) - x(t)\| = 0,$$

and

$$\|y(t) - x(t)\| = 0, \quad \text{for all } t \ge T_{finite-time}.$$

Here, the synchronization settling time is defined as: $T_0 = \inf\{T_{finite-time} \ge 0 : x(t) = y(t) \quad \text{for all } t \ge T_{finite-time}\}$.

Definition 5 *The drive FRCohGNNs (1) and the response FRCohGNNs (2) are said to achieve fixed-time synchronization if there exists a constant $T_{fixed-time} \ge 0$, independent of the initial conditions, such that for any initial conditions $\phi_i(t)$ and $\varphi_i(t)$, the following holds:*

$$\lim_{t \to T_{fixed-time}} \|y(t) - x(t)\| = 0, \ \forall \phi_i, \ \varphi_i \in \mathbb{R},$$

and

$$\|y(t) - x(t)\| = 0, \quad \text{for all } t \ge T_{fixed-time}.$$

This means the synchronization occurs within the fixed time $T_{fixed-time}$, regardless of the initial states.

Definition 6 *The drive FRCohGNNs (1) and the response FRCohGNNs (2) are said to achieve P_fT synchronization if they satisfy the conditions for fixed-time synchronization, and their settling time is bounded by a preset constant $T^P > 0$. Hence, for any initial conditions $\phi_i(t)$ and $\varphi_i(t)$, the synchronization time $T_{finite-time}$ satisfies:*

$$T_{finite-time} \le T^P.$$

In other words, the systems synchronize within a fixed time T^P, which is chosen in advance and does not depend on the initial states.

Remark 2 *The study of synchronization between two systems within a P_fT is equivalent to analyzing the P_fT stability of the error system. Specifically, consider the error dynamics (3) derived from systems (1) and (2). When the error dynamics achieve P_fT stability at the origin, the global synchronization of systems (1) and (2) is ensured within the specified P_fT.*

Lemma 1 [31] *Consider a continuous differentiable function $V(\cdot) : \mathbb{R}^n \to \mathbb{R}_+ \cup \{0\}$ satisfying the following conditions:*

1. *$V(x(t)) = 0$ if and only if $x(t) = 0$;*
2. *If $\|x(t)\| \to +\infty$, then $V(x(t)) \to +\infty$;*
3. *For any $x(t) \in \mathbb{R}^n$ and any $T^P > 0$, there exist positive constants $0 < q < 1$ such that:*

$$\dot{V}(x(t)) \leq -\frac{\pi}{qT^P}\left(V(x(t))^{1-\frac{q}{2}} + V(x(t))^{1+\frac{q}{2}}\right),$$

Then, the equilibrium point $x(t) = 0$ is P_fT stable, and T^p is the predefined settling time.

Lemma 2 [32] *Consider the error system (3). Suppose there exists a Lyapunov function $V(t)$ that satisfies the following inequality:*

$${}_0D_t^{\alpha}V(t) \leq -\frac{1}{T_c^{\alpha}}\left(\Sigma_1 V^{r_1}(t) + \Sigma_2 V^{r_2}(t)\right),$$

where $T_c > 0$ is a predefined time constant and T_c^{α} denotes its α-th power. The exponents and constants satisfy:

$$1 < r_1 < 1 + \alpha, \quad 0 < r_2 < \alpha < 1,$$

where $\Sigma_1 = \dfrac{-2^{\alpha}(1-r_1)\Gamma(1+\alpha-r_1)}{\Gamma(2-r_1)\Gamma(1+\alpha)}$,
$\Sigma_2 = \dfrac{2^{\alpha}\Gamma(1+\alpha-r_2)}{\Gamma(1-r_2)\Gamma(1+\alpha)}$.
Then, the error system is P_fT stable, with T_c as the settling time determined in advance.

Lemma 3 [32] *Let $x_i \geq 0$, $0 < q < 1$, and $p > 1$. Then, the following inequalities hold:*
$x_1^q + x_2^q + \cdots + x_n^q \geq (x_1 + x_2 + \cdots + x_n)^q$,
and
$x_1^p + x_2^p + \cdots + x_n^p \geq n^{1-p}(x_1 + x_2 + \cdots + x_n)^p$.

Lemma 4 [33] *Let $\hbar(t) \in C^1([t_0, +\infty), \mathbb{R})$ be a continuously differentiable function. For any fractional order $\gamma \in (0, 1)$ and for almost every $t \geq t_0$, the following inequality holds :*

$$D^{\gamma}|\hbar(t)| \leq \operatorname{sgn}\big(\hbar(t)\big)\, D^{\gamma}\hbar(t),$$

where $\operatorname{sgn}(\cdot)$ is the sign function.

Lemma 5 [36] *Suppose that $\hbar(t) \in C^1[0, T]$. Therefore,*

$$D^{\beta_1}D^{\beta_2}\hbar(t) = D^{\beta_1+\beta_2}\hbar(t),$$

where $\beta_1, \beta_2 > 0$ and $\beta_1 + \beta_2 \leq 1$; T is a positive constant.

Remark 3 *The parameters γ and δ in the drive–response systems (1) and (2) are not necessarily aligned, they may be equal or different, which increases the difficulty of achieving synchronization [34]. Moreover, even slight variations in the system orders can significantly influence the dynamic behavior of FRCohGNNs, providing a wider range of possibilities for designing chaotic encryption schemes. For these reasons, this work investigates the P_fT of FRCohGNNs with distinct-order γ and δ. This analysis represents a meaningful contribution, as it addresses a challenging configuration that has received limited attention in the current literature.*

3 Main results

By applying the above lemmas and assumptions, P_fT synchronization of the drive–response (1)-(2) systems are achieved in this section. We now introduce the following P_fT controllers designed to achieve synchronization within a predefined time

$$U_{1i,2i}(t) = U_{1i}(t) + U_{2i}(t), \tag{4}$$

where

$$\begin{cases} U_{1i}(t) &= -\zeta_{1i}\,|\epsilon_i(t)| - D^{\delta-1}\big\{sgn(\epsilon_i(t)) \\ &\times \left(\eta_1|\epsilon_i(t)|^{1+q} + \eta_2|\epsilon_i(t)|^{1-q}\right)\big\} \\ &- \alpha_i\left(x_i(t)\right)\sum_{j=1}^{n} c_{ij}\Big(g_j\left(y_j(t)\right) \\ &- g_j\left(x_j(t)\right)\Big) \\ &- \alpha_i\left(x_i(t)\right)\sum_{j=1}^{n} d_{ij}\Big(h_j\left(y_j(t-\sigma(t))\right) \\ &- h_j\left(x_j(t-\sigma(t))\right)\Big), \\ U_{2i}(t) &= D_i^{\delta}x_i(t) - D_i^{\gamma}x_i(t), \end{cases} \tag{5}$$

where, $i = 1, 2, \cdots, n$, $\eta_1 = \dfrac{n^{\frac{q}{2}}\pi}{T^P 2^{(1+\frac{q}{2})}q}$, $\eta_2 = \dfrac{\pi}{T^P 2^{(1-\frac{q}{2})}q}$, and ζ_{1i} is a positive constant.

Theorem 1 *Under hypotheses (**H1**)-(**H3**) with controller (4), if the condition*

$$\zeta_{1i} \geq \varpi_i + \lambda_i\sum_{j=1}^{n}|c_{ij}|G_j + \lambda_i\sum_{j=1}^{n}|d_{ij}|H_j + I_i\lambda_i, \tag{6}$$

holds, then the drive system (1) and response system (2) of the FRCohGNNs model reach synchronization within the predefined time T^P.

Proof 1 *The Lyapunov candidate function is selected as*

$$V(\epsilon(t)) = \frac{1}{2}\sum_{i=1}^{n}\epsilon_i^2(t) \tag{7}$$

Based on Lemma 5 and by computing the time derivative of the Lyapunov function, we get

$$\begin{aligned}
\dot{V}(\epsilon(t)) &= \sum_{i=1}^{n}\epsilon_i(t)\dot{\epsilon}_i(t)\\
&= \sum_{i=1}^{n}\epsilon_i(t)D^{1-\delta}(D^{\delta}\epsilon_i(t))\\
&= \sum_{i=1}^{n}\epsilon_i(t)D^{1-\delta}\Big[-\alpha_i\left(y_i(t)\right)\Big(\beta_i\left(y_i(t)\right)\\
&- \sum_{j=1}^{n}c_{ij}g_j\left(y_j(t)\right) - \sum_{j=1}^{n}d_{ij}h_j\left(y_j(t-\sigma(t))\right)\\
&- I_i\Big) + \alpha_i\left(x_i(t)\right)\Big(\beta_i\left(x_i(t)\right)\\
&- \sum_{j=1}^{n}c_{ij}g_j\left(x_j(t)\right) - \sum_{j=1}^{n}d_{ij}h_j\left(x_j(t-\sigma(t))\right)\\
&- I_i\Big) - D_i^{\delta}x_i(t) + D_i^{\gamma}x_i(t) + U_{1i,2i}(t)\Big]\\
&= \sum_{i=1}^{n}\epsilon_i(t)D^{1-\delta}\Big[-\alpha_i\left(y_i(t)\right)\Big(\beta_i\left(y_i(t)\right)\\
&- \sum_{j=1}^{n}c_{ij}g_j\left(y_j(t)\right) - \sum_{j=1}^{n}d_{ij}h_j\left(y_j(t-\sigma(t))\right)\\
&- I_i\Big) + \alpha_i\left(x_i(t)\right)\Big(\beta_i\left(x_i(t)\right)\\
&- \sum_{j=1}^{n}c_{ij}g_j\left(x_j(t)\right) - \sum_{j=1}^{n}d_{ij}h_j\left(x_j(t-\sigma(t))\right)\\
&- I_i\Big) + U_{1i}(t)\Big].
\end{aligned} \tag{8}$$

*According to (**H3**), it is clear that*

$$\begin{aligned}
\dot{V}(\epsilon(t)) &\leq \sum_{i=1}^{n}\epsilon_i(t)D^{1-\delta}\Big[\varpi_i|\epsilon_i(t)| + \sum_{j=1}^{n}\Big(\alpha_i\left(y_i(t)\right)\\
&- \alpha_i\left(x_i(t)\right)\Big)c_{ij}g_j\left(y_j(t)\right)\\
&+ \sum_{j=1}^{n}\alpha_i\left(x_i(t)\right)\left(c_{ij}g_j\left(y_j(t)\right) - c_{ij}g_j\left(x_j(t)\right)\right)\\
&+ \sum_{j=1}^{n}\left(\alpha_i\left(y_i(t)\right) - \alpha_i\left(x_i(t)\right)\right)\\
&\times d_{ij}h_j\left(y_j(t-\sigma(t))\right)\\
&+ \sum_{j=1}^{n}\alpha_i\left(x_i(t)\right)\Big(d_{ij}h_j\left(y_j(t-\sigma(t))\right)\\
&- d_{ij}h_j\left(x_j(t-\sigma(t))\right)\Big)\\
&+ I_i\Big(\alpha_i\left(y_i(t)\right) - \alpha_i\left(x_i(t)\right)\Big) + U_{1i}(t)\Big].
\end{aligned} \tag{9}$$

*By (**H1**) and (**H2**), we have*

$$\begin{aligned}
\dot{V}(\epsilon(t)) &\leq \sum_{i=1}^{n}\epsilon_i(t)D^{1-\delta}\Big[\Big(-\zeta_{1i} + \varpi_i\\
&+ \lambda_i\sum_{j=1}^{n}|c_{ij}|G_j + \lambda_i\sum_{j=1}^{n}|d_{ij}|H_j\\
&+ I_i\lambda_i\Big)|\epsilon_i(t)|\\
&- D^{\delta-1}\Big(sgn(\epsilon_i(t))\Big(\eta_1|\epsilon_i(t)|^{1+q}\\
&+ \eta_2|\epsilon_i(t)|^{1-q}\Big)\Big)\Big].
\end{aligned} \tag{10}$$

From (6) and Proposition 1, one obtains

$$\begin{aligned}
\dot{V}(\epsilon(t)) &\leq -\sum_{i=1}^{n}\epsilon_i(t)D^{1-\delta}\Big[D^{\delta-1}\Big(sgn(\epsilon_i(t))\\
&\times \left(\eta_1|\epsilon_i(t)|^{1+q} + \eta_2|\epsilon_i(t)|^{1-q}\right)\Big)\Big]\\
&= -\sum_{i=1}^{n}\left(\eta_1|\epsilon_i(t)|^{2+q} + \eta_2|\epsilon_i(t)|^{2-q}\right)\\
&= -\eta_1\sum_{i=1}^{n}\left(|\epsilon_i(t)|^2\right)^{\frac{2+q}{2}}\\
&- \eta_2\sum_{i=1}^{n}\left(|\epsilon_i(t)|^2\right)^{\frac{2-q}{2}}.
\end{aligned} \tag{11}$$

Based on Lemma 3, it follows that

$$\begin{aligned}\dot{V}(\epsilon(t)) &\leq -\eta_1\left(\sum_{i=1}^{n}\epsilon_i^2(t)\right)^{1+\frac{q}{2}} - \eta_2\left(\sum_{i=1}^{n}\epsilon_i^2(t)\right)^{1-\frac{q}{2}} \\ &\leq -\eta_1 n^{-\frac{q}{2}} 2^{1+\frac{q}{2}} V(t)^{1+\frac{q}{2}} - \eta_2 2^{1-\frac{q}{2}} V(t)^{1-\frac{q}{2}} \\ &= -\frac{\pi}{qT^P}\left(V(t)^{1+\frac{q}{2}} + V(t)^{1-\frac{q}{2}}\right). \end{aligned} \tag{12}$$

Lemma 1 ensures that $\epsilon_i(t) = 0$ is stable in predefined time, with T^P representing the corresponding predefined settling time.

Remark 4 *Theorem 1 utilizes the conventional Lyapunov direct method with integer-order differentiation $\dot{V}$ to examine the stability of fractional-order systems. In contrast, we now adopt the fractional-order Lyapunov direct method, denoted by $D^\delta V$, which is more appropriate for fractional-order systems and helps to eliminate differentiation-related inaccuracies.*

To ensure P_fT synchronization between the FRCohGNNs described in (1) and (2), and based on Lemma 2, the following controllers are incorporated into the slave system (2), which is expressed as

$$U_{1i,2i}(t) = U_{1i}(t) + U_{2i}(t), \tag{13}$$

where

$$\begin{cases} U_{1i}(t) &= -\zeta_{2i}\epsilon_i(t) - sgn(\epsilon_i(t))\Big(\zeta_{3i}|\epsilon_i(t-\sigma(t))| \\ &+ \eta_3|\epsilon_i(t)|^{r_1} + \eta_4|\epsilon_i(t)|^{r_2}\Big), \\ U_{2i}(t) &= D^\delta x_i(t) - D^\gamma x_i(t), \end{cases}$$

where ζ_{2i}, and ζ_{3i} are constants that will be specified later, and the parameters η_3 and η_4 are defined as

$$\eta_3 = \frac{\Sigma_1}{T^P n^{1-r_1}}, \quad \eta_4 = \frac{\Sigma_2}{T^P},$$

where

$$\Sigma_1 = \frac{-2^\delta(1-r_1)\Gamma(1+\delta-r_1)}{\Gamma(2-r_1)\Gamma(1+\delta)}, \quad \Sigma_2 = \frac{2^\delta\Gamma(1+\delta-r_2)}{\Gamma(1-r_2)\Gamma(1+\delta)}.$$

with $1 < r_1 < 1+\delta$, $0 < r_2 < \delta < 1$, and indices $i = 1, 2, \ldots, n$.

Theorem 2 *Assume that Assumptions (**H1**)–(**H3**) are satisfied and that controller (13) is applied. If the following inequalities are satisfied:*

$$\begin{cases} \zeta_{2i} &\geq \varpi_i + \sum_{j=1}^{n}\lambda_i|c_{ij}|G_j + \sum_{j=1}^{n}\overline{\alpha}_j|c_{ji}|L_i^g \\ &+ \sum_{j=1}^{n}\lambda_i|d_{ij}|H_j + \lambda_i I_i, \\ \zeta_{3i} &\geq \sum_{j=1}^{n}\overline{\alpha}_j|d_{ji}|L_i^h, \end{cases} \tag{14}$$

then the P_fT synchronization of the systems (1) and (2) is guaranteed, with convergence time T^P.

Proof 2 *First, we introduce the following Lyapunov function constructed on the L_1-norm:*

$$V(\epsilon(t)) = \sum_{i=1}^{n}|\epsilon_i(t)|. \tag{15}$$

According to Lemma 4, we can show that

$$D^\delta|\epsilon_i(t)| \leq \operatorname{sgn}(\epsilon_i(t))\, D^\delta\epsilon_i(t).$$

Therefore, for the Lyapunov function given in (15), it follows that

$$\begin{aligned} D^\delta V(\epsilon(t)) &= \sum_{i=1}^{n} D^\delta|\epsilon_i(t)| \\ &\leq \sum_{i=1}^{n}\operatorname{sgn}(\epsilon_i(t))\, D^\delta\epsilon_i(t) \\ &= \sum_{i=1}^{n}\operatorname{sgn}(\epsilon_i(t))\Big(-\alpha_i(y_i(t))\Big(\beta_i(y_i(t)) \\ &- \sum_{j=1}^{n}c_{ij}g_j(y_j(t)) - \sum_{j=1}^{n}d_{ij}h_j(y_j(t-\sigma(t))) \\ &- I_i\Big) + \alpha_i(x_i(t))\Big(\beta_i(x_i(t)) \\ &- \sum_{j=1}^{n}c_{ij}g_j(x_j(t)) \\ &- \sum_{j=1}^{n}d_{ij}h_j(x_j(t-\sigma(t))) - I_i\Big) \\ &+ U_{1i}(t)\Big) \\ &= \sum_{i=1}^{n}\operatorname{sgn}(\epsilon_i(t))\Big((\alpha_i(x_i(t))\beta_i(x_i(t)) \\ &- \alpha_i(y_i(t))\beta_i(y_i(t))) \\ &+ \sum_{j=1}^{n}\big(\alpha_i(y_i(t)) - \alpha_i(x_i(t))\big)c_{ij}g_j(y_j(t)) \\ &+ \sum_{j=1}^{n}\alpha_i(x_i(t))\big(c_{ij}g_j(y_j(t)) - c_{ij}g_j(x_j(t))\big) \\ &+ \sum_{j=1}^{n}\big(\alpha_i(y_i(t)) - \alpha_i(x_i(t))\big) \\ &\times d_{ij}h_j(y_j(t-\sigma(t))) \\ &+ \sum_{j=1}^{n}\alpha_i(x_i(t))\big(d_{ij}h_j(y_j(t-\sigma(t))) \\ &- d_{ij}h_j(x_j(t-\sigma(t)))\big) \\ &+ I_i\big(\alpha_i(y_i(t)) - \alpha_i(x_i(t))\big) + U_{1i}(t)\Big) \end{aligned} \tag{16}$$

*From (**H1**)–(**H3**), it follows that*

$$\begin{aligned}
D^{\delta}V(\epsilon(t)) &\leq \sum_{i=1}^{n}\varpi_i|\epsilon_i(t)| + \sum_{i=1}^{n}\sum_{j=1}^{n}\lambda_i|\epsilon_i(t)||c_{ij}|G_j \\
&+ \sum_{i=1}^{n}\sum_{j=1}^{n}\overline{\alpha}_i|c_{ij}|L_j^g|\epsilon_j(t)| \\
&+ \sum_{i=1}^{n}\sum_{j=1}^{n}\lambda_i|\epsilon_i(t)||d_{ij}|H_j \\
&+ \sum_{i=1}^{n}\sum_{j=1}^{n}\overline{\alpha}_i|d_{ij}|L_j^h|\epsilon_j(t-\sigma(t))| \\
&+ \lambda_i I_i|\epsilon_i(t)| - \sum_{i=1}^{n}\zeta_{2i}|\epsilon_i(t)| \\
&- \sum_{i=1}^{n}\Big(\zeta_{3i}|\epsilon_i(t-\sigma(t))| + \eta_3|\epsilon_i(t)|^{r_1} \\
&+ \eta_4|\epsilon_i(t)|^{r_2}\Big)\Big) \\
&= \sum_{i=1}^{n}\varpi_i|\epsilon_i(t)| + \sum_{i=1}^{n}\sum_{j=1}^{n}\lambda_i|\epsilon_i(t)||c_{ij}|G_j \\
&+ \sum_{i=1}^{n}\sum_{j=1}^{n}\overline{\alpha}_j|c_{ji}|L_i^g|\epsilon_i(t)| \\
&+ \sum_{i=1}^{n}\sum_{j=1}^{n}\lambda_i|\epsilon_i(t)||d_{ij}|H_j \\
&+ \sum_{i=1}^{n}\sum_{j=1}^{n}\overline{\alpha}_j|d_{ji}|L_i^h|\epsilon_i(t-\sigma(t))| \\
&+ \lambda_i I_i|\epsilon_i(t)| - \sum_{i=1}^{n}\zeta_{2i}|\epsilon_i(t)| \\
&- \sum_{i=1}^{n}\Big(\zeta_{3i}|\epsilon_i(t-\sigma(t))| + \eta_3|\epsilon_i(t)|^{r_1} \\
&+ \eta_4|\epsilon_i(t)|^{r_2}\Big)\Big) \\
&= \sum_{i=1}^{n}\Big[-\zeta_{2i} + \varpi_i + \sum_{j=1}^{n}\lambda_i|c_{ij}|G_j \\
&+ \sum_{j=1}^{n}\overline{\alpha}_j|c_{ji}|L_i^g + \sum_{j=1}^{n}\lambda_i|d_{ij}|H_j \\
&+ \lambda_i I_i\Big]|\epsilon_i(t)| + \sum_{i=1}^{n}\Big[-\zeta_{3i} \\
&+ \sum_{j=1}^{n}\overline{\alpha}_j|d_{ji}|L_i^h\Big]|\epsilon_i(t-\sigma(t))| \\
&- \sum_{i=1}^{n}\Big[\eta_3|\epsilon_i(t)|^{r_1} + \eta_4|\epsilon_i(t)|^{r_2}\Big]. \qquad (17)
\end{aligned}$$

By applying the inequality condition (14), we obtain:

$$D^{\delta}V(\epsilon(t)) \leq -\eta_3\sum_{i=1}^{n}|\epsilon_i(t)|^{r_1} - \eta_4\sum_{i=1}^{n}|\epsilon_i(t)|^{r_2}. \qquad (18)$$

According to Lemma 3, the following inequality can be derived

$$\begin{aligned}
D^{\delta}V(\epsilon(t)) &\leq -\eta_3 n^{1-r_1}\Big(\sum_{i=1}^{n}|\epsilon_i(t)|\Big)^{r_1} \\
&- \eta_4\Big(\sum_{i=1}^{n}|\epsilon_i(t)|\Big)^{r_2} \\
&= -\eta_3 n^{1-r_1}V(t)^{r_1} - \eta_4 V(t)^{r_2} \\
&= -\frac{\Sigma_1}{T^P}V(t)^{r_1} - \frac{\Sigma_2}{T^P}V(t)^{r_2}. \qquad (19)
\end{aligned}$$

According to Lemma 4, the error term $\epsilon_i(t)$ converges to zero within the predefined time T^P.

Remark 5 *References [16–19, 21, 23] investigate the drive–response synchronization of CohGNNs, mainly focusing on fixed-time and finite-time synchronization, while Theorems 1 and 2 considers predefined-time synchronization. It is worth noting that these works consider systems without fractional order, while in this paper the fractional-order case is investigated. Consequently, this work extends previous studies, especially [16–19, 21, 23].*

4 Numerical examples

To confirm the accuracy of the proposed theoretical results, two illustrative examples are provided in this section.

Example 1

Consider a delayed FRCohGNNs model described by the following master system:

$$\begin{aligned}
D_i^{\gamma}x_i(t) &= -\alpha_i\left(x_i(t)\right)\Big(\beta_i\left(x_i(t)\right) \\
&- \sum_{j=1}^{2}c_{ij}g_j\left(x_j(t)\right) - \sum_{j=1}^{2}d_{ij}h_j\left(x_j(t-\sigma(t))\right) \\
&- I_i\Big), \qquad (20)
\end{aligned}$$

and the corresponding slave system:

$$\begin{aligned} D_i^{\delta} y_i(t) &= -\alpha_i\left(y_i(t)\right)\Big(\beta_i\left(y_i(t)\right) \\ &- \sum_{j=1}^{2} c_{ij} g_j\left(y_j(t)\right) - \sum_{j=1}^{2} d_{ij} h_j\left(y_j(t-\sigma(t))\right) \\ &- I_i\Big) + U_{1i,2i}(t), \end{aligned} \tag{21}$$

The system parameters are defined as follows:

$$\begin{aligned} &\gamma = 0.98,\ \delta = 0.96, \alpha_1(x) = \alpha_2(x) = 0.3 + \frac{0.1}{1+x^2}, \\ &\beta_1(x) = \beta_2(x) = 0.4x, \\ &g_1(x) = g_2(x) = \sin(2.3x), \\ &h_1(x) = h_2(x) = \sin(2.2x), \\ &\sigma(t) = 0.8 + 0.2\sin(t), \quad I_1 = I_2 = 1, \\ &c_{11} = 1.4, c_{12} = 1.9, c_{21} = 2.4, c_{22} = 0.9, \\ &d_{11} = 2.9, d_{12} = 2.2, d_{21} = 1.8, d_{22} = 1.9. \end{aligned}$$

The initial conditions are selected as:
$x_1(0) = 0.5,\ x_2(0) = -0.5,\ y_1(0) = 2,\ y_2(0) = -2.$

Based on the given functions and parameters, we obtain:

$$\begin{aligned} &G_1 = G_2 = H_1 = H_2 = 1, \quad L_1^g = L_2^g = 2.3, \\ &L_1^h = L_2^h = 2.2, \\ &\underline{\alpha}_1 = \underline{\alpha}_2 = 0.3, \quad \overline{\alpha}_1 = \overline{\alpha}_2 = 0.4, \\ &\lambda_1 = \lambda_2 = 0.05, \quad \varpi_1 = \varpi_2 = 0.16. \end{aligned}$$

The numerical simulation results of system (20) are illustrated in Figures 1 and 2.

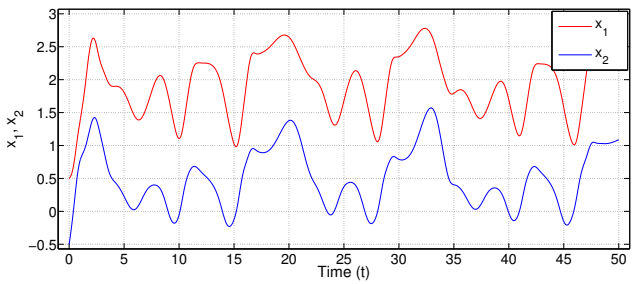

Figure 1. Time evolution of states $x_1(t)$ and $x_2(t)$ in system (20).

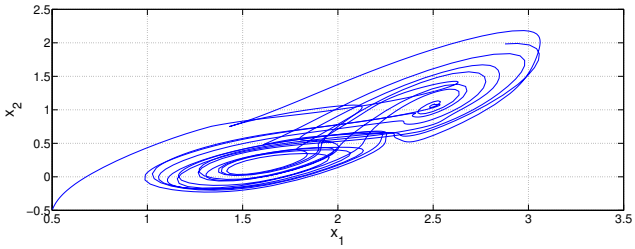

Figure 2. The phase diagram of system (20).

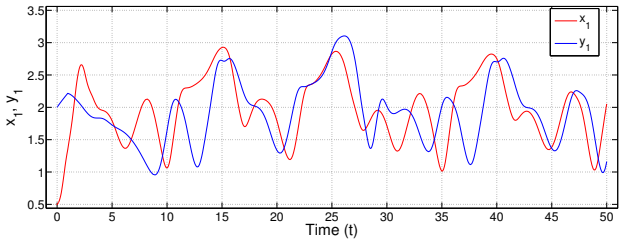

Figure 3. The state responses $x_1(t)$ and $y_1(t)$ without the application of control law (22).

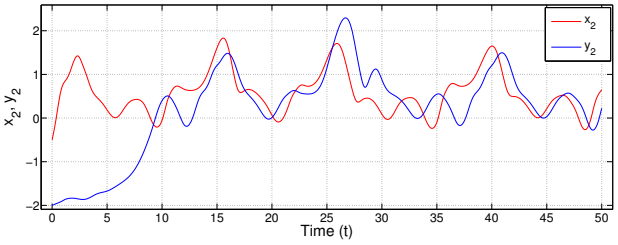

Figure 4. The state responses $x_2(t)$ and $y_2(t)$ without the application of control law (22).

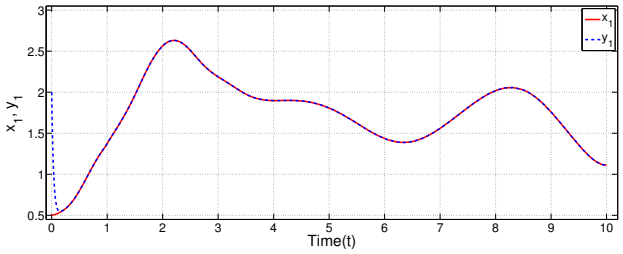

Figure 5. The state responses $x_1(t)$ and $y_1(t)$ under the application of control law (22).

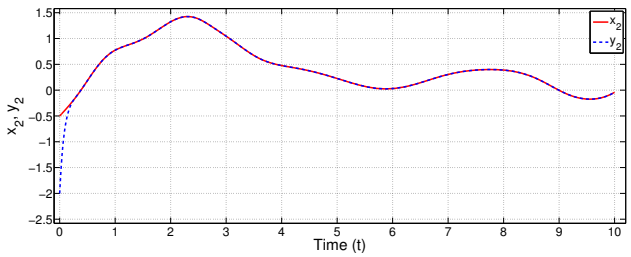

Figure 6. The state responses $x_2(t)$ and $y_2(t)$ under the application of control law (22).

Next, let us select the parameters $\zeta_{11} = 0.70, \zeta_{12} = 0.60$, $T^P = 0.5$, $\eta_1 = 10.47197551$, $\eta_2 = 11.61938434$, and $q = 0.3$ and proceed to verify the conditions stated in Theorem 1. Under these parameter settings, we obtain

$$\begin{cases} \zeta_{11} = 0.70 & \geq & \varpi_1 + \lambda_1 \sum_{j=1}^{2} |c_{1j}| G_j + \lambda_1 \sum_{j=1}^{2} |d_{1j}| H_j \\ & + & I_1 \lambda_1 = 0.63, \\ \zeta_{12} = 0.60 & \geq & \varpi_2 + \lambda_2 \sum_{j=1}^{2} |c_{2j}| G_j + \lambda_2 \sum_{j=1}^{2} |d_{2j}| H_j \\ & + & I_2 \lambda_2 = 0.56, \end{cases}$$

Therefore, the selected parameters satisfy the sufficient conditions of Theorem 1. The controller is accordingly defined by:

$$U_{1i,2i}(t) = U_{1i}(t) + U_{2i}(t), \ i = 1, 2, \tag{22}$$

where

$$\begin{cases} U_{11}(t) & = & -\zeta_{11} |\epsilon_1(t)| - D^{\delta-1} \Big\{ sgn(\epsilon_1(t)) \Big(\eta_1 |\epsilon_1(t)|^{1+q} \\ & + & \eta_2 |\epsilon_1(t)|^{1-q} \Big) \Big\} \\ & - & \alpha_1 (x_1(t)) \sum_{j=1}^{2} c_{1j} \big(g_j (y_j(t)) - g_j (x_j(t)) \big) \\ & - & \alpha_1 (x_i(t)) \sum_{j=1}^{2} d_{1j} \big(h_j (y_j(t - \sigma(t))) \\ & - & h_j (x_j(t - \sigma(t))) \big), \\ U_{12}(t) & = & -\zeta_{12} |\epsilon_2(t)| - D^{\delta-1} \Big\{ sgn(\epsilon_2(t)) \\ & \times & \big(\eta_1 |\epsilon_2(t)|^{1+q} + \eta_2 |\epsilon_2(t)|^{1-q} \big) \Big\} \\ & - & \alpha_2 (x_2(t)) \sum_{j=1}^{n} c_{2j} \big(g_j (y_j(t)) - g_j (x_j(t)) \big) \\ & - & \alpha_2 (x_2(t)) \sum_{j=1}^{n} d_{2j} \big(h_j (y_j(t - \sigma(t))) \\ & - & h_j (x_j(t - \sigma(t))) \big), \\ U_{21}(t) & = & D^{\delta} x_1(t) - D^{\gamma} x_1(t), \\ U_{22}(t) & = & D^{\delta} x_2(t) - D^{\gamma} x_2(t), \end{cases} \tag{23}$$

With and without control (22), the transient dynamics of the state variables for systems (20) and (21) are presented in Figures 3, 4, 5 and 6. Furthermore, the synchronization errors $\epsilon_i(t), i = 1, 2$ are shown in Figure 7. The results confirm that synchronization between the master system (20) and the slave system (21) is achieved within predefined time $T^P = 0.5$, and the convergence error remains zero afterward. These simulation outcomes corroborate the theoretical results obtained earlier.

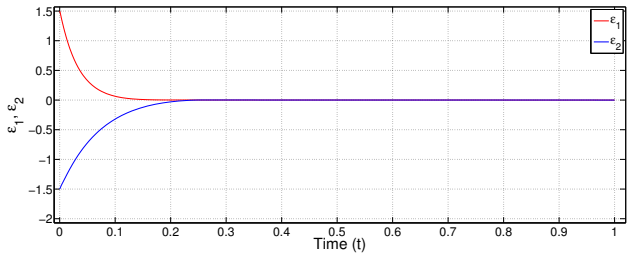

Figure 7. Synchronization errors $\epsilon_1(t)$ and $\epsilon_2(t)$ under control (22) with $T^P = 0.5$.

Next, we will modify the time T^P to values 2 and 0.1 to investigate the validity of control (22), as shown in Figures 8 and 9, respectively.

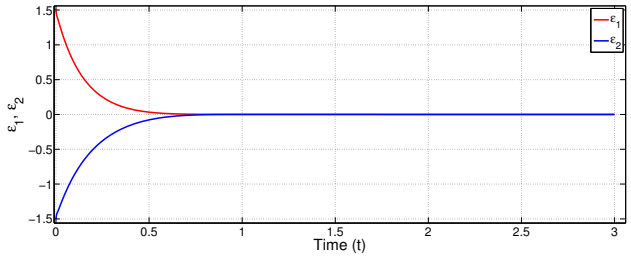

Figure 8. Synchronization errors $\epsilon_1(t)$ and $\epsilon_2(t)$ under control (22) with $T^P = 2$.

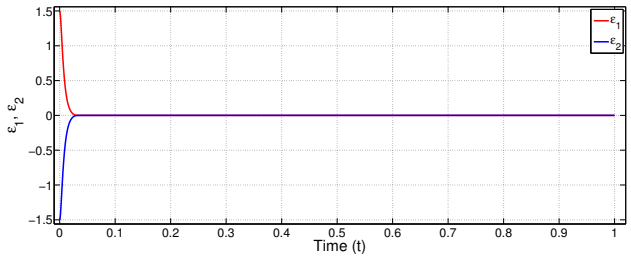

Figure 9. Synchronization errors $\epsilon_1(t)$ and $\epsilon_2(t)$ under control (22) with $T^P = 0.1$.

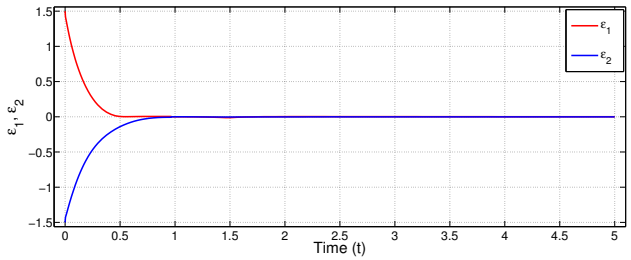

Figure 10. Synchronization errors $\epsilon_1(t)$ and $\epsilon_2(t)$ under control (24) with $T^P = 2$.

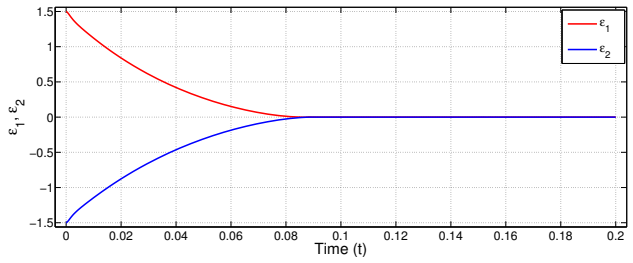

Figure 11. Synchronization errors $\epsilon_1(t)$ and $\epsilon_2(t)$ under control (24) with $T^P = 0.1$.

Example 2

In continuation of Example 1, the control scheme (22) is modified to (24). Let $\zeta_{21} = 4.50$, $\zeta_{22} = 3.50$, $\zeta_{31} = 4.50$, $\zeta_{32} = 4.50$, $\eta_3 = \frac{0.4118}{T^P 2^{(-0.2)}}$, $\eta_4 = \frac{1.3736}{T^P}$, $r_1 = 1.2$ and $r_2 = 0.3$, the following result is obtained

$$\begin{cases} \zeta_{21} = 4.50 & \geq & \varpi_1 + \sum_{j=1}^{2} \lambda_1 |c_{1j}| G_j \\ & + & \sum_{j=1}^{n} \overline{\alpha}_j |c_{j1}| L_1^g + \sum_{j=1}^{n} \lambda_1 |d_{1j}| H_j \\ & + & \lambda_1 I_1 = 4.126, \\ \zeta_{22} = 3.50 & \geq & \varpi_2 + \sum_{j=1}^{n} \lambda_2 |c_{2j}| G_j \\ & + & \sum_{j=1}^{n} \overline{\alpha}_j |c_{j2}| L_2^g + \sum_{j=1}^{n} \lambda_2 |d_{2j}| H_j \\ & + & \lambda_2 I_2 = 3.136, \\ \zeta_{31} = 4.50 & \geq & \sum_{j=1}^{2} \overline{\alpha}_j |d_{j1}| L_1^h = 4.136, \\ \zeta_{32} = 4.50 & \geq & \sum_{j=1}^{2} \overline{\alpha}_j |d_{j2}| L_2^h = 3.608. \end{cases}$$

Based on Theorem 2, synchronization between the response system (21) and the drive system (20) is attained in the predefined time $T^P = 2$ and $T^P = 0.1$ using controller

$$\begin{cases} U_{11}(t) & = & -\zeta_{21}\epsilon_1(t) - sgn(\epsilon_1(t)) \\ & \times & \Big(\zeta_{31} |\epsilon_1(t - \sigma(t))| \\ & + & \eta_3 |\epsilon_1(t)|^{r_1} + \eta_4 |\epsilon_1(t)|^{r_2} \Big), \\ U_{12}(t) & = & -\zeta_{22}\epsilon_2(t) - sgn(\epsilon_2(t)) \\ & \times & \Big(\zeta_{32} |\epsilon_2(t - \sigma(t))| \\ & + & \eta_3 |\epsilon_2(t)|^{r_1} + \eta_4 |\epsilon_2(t)|^{r_2} \Big), \\ U_{21}(t) & = & D^{\delta} x_1(t) - D^{\gamma} x_1(t), \\ U_{22}(t) & = & D^{\delta} x_2(t) - D^{\gamma} x_2(t). \end{cases} \tag{24}$$

The evolution of synchronization errors for the drive and response systems (20)-(21) is depicted in Figures 10 and 11.

Remark 6 *From Examples 1 and 2, we can see that the fractional neural networks with delays reach synchronization within the predefined time T^P, regardless of the initial conditions. The predefined time T^P can be chosen as a specific parameter in the predefined-time controllers, meaning it can take any positive value (see Figures 7–11). Based on real-world requirements, the predefined time T^P, which represents the maximum synchronization time, can be adjusted freely. For this reason, predefined-time synchronization is more advantageous than traditional methods such as asymptotic or finite-time synchronization and fixed-time synchronization.*

5 Conclusion and Future Work

In this paper, we investigated the $P_f T$ synchronization problem for distinct-order FRCohGNNs with time-varying delays. Two control strategies were proposed: one using a fractional-order controller and another using a standard controller. Based on Lyapunov theory and properties of fractional calculus, sufficient conditions were derived to ensure synchronization within a predefined time, regardless of the initial conditions. Numerical simulations confirmed the effectiveness of the proposed methods.

As future work, we plan to extend this study to more complex neural network models, such as stochastic FRCohGNNs and bidirectional associative memory (BAM) neural networks. In addition, exploring synchronization under uncertain environments and external disturbances remains an interesting direction for future research.

Data Availability Statement

Data will be made available on request.

Funding

This work was supported without any funding.

Conflicts of Interest

The authors declare no conflicts of interest.

Ethical Approval and Consent to Participate

Not applicable.

References

[1] Morita, M. (1993). Associative memory with nonmonotone dynamics. *Neural Networks, 6*(1), 115–126. [CrossRef]

[2] Alimi, A. M., Aouiti, C., & Assali, E. A. (2019). Finite-time and fixed-time synchronization of a class of inertial neural networks with multi-proportional delays and its application to secure communication. *Neurocomputing, 332*, 29–43. [CrossRef]

[3] Melin, P., Mendoza, O., & Castillo, O. (2011). Face recognition with an improved interval type-2 fuzzy logic sugeno integral and modular neural networks. *IEEE Transactions on systems, man, and cybernetics-Part A: systems and humans, 41*(5), 1001-1012. [CrossRef]

[4] Lai, Q., Wan, Z., Zhang, H., & Chen, G. (2022). Design and analysis of multiscroll memristive Hopfield neural network with adjustable memductance and application to image encryption. *IEEE Transactions on Neural Networks and Learning Systems, 34*(10), 7824-7837. [CrossRef]

[5] Aouiti, C., & Dridi, F. (2020). New results on interval general Cohen-Grossberg BAM neural networks. *Journal of Systems Science and Complexity, 33*(4), 944–967. [CrossRef]

[6] Li, R., Gao, X., Cao, J., & Zhang, K. (2019). Stability analysis of quaternion-valued Cohen-Grossberg neural networks. *Mathematical Methods in the Applied Sciences, 42*(10), 3721–3738. [CrossRef]

[7] Peng, D., Li, X., Aouiti, C., & Miaadi, F. (2018). Finite-time synchronization for Cohen–Grossberg neural networks with mixed time-delays. *Neurocomputing, 294*, 39–47. [CrossRef]

[8] Cohen, M. A., & Grossberg, S. (1983). Absolute stability of global pattern formation and parallel memory storage by competitive neural networks. *IEEE transactions on systems, man, and cybernetics*, (5), 815-826. [CrossRef]

[9] Li, P., Gao, R., Xu, C., Shen, J., Ahmad, S., & Li, Y. (2023). Exploring the impact of delay on Hopf bifurcation of a type of BAM neural network models concerning three nonidentical delays. *Neural Processing Letters, 55*(8), 11595–11635. [CrossRef]

[10] Li, Q., Wei, H., Hua, D., Wang, J., & Yang, J. (2024). Stabilization of semi-Markovian jumping uncertain complex-valued networks with time-varying delay: A sliding-mode control approach. *Neural Processing Letters, 56*(2), 111. [CrossRef]

[11] Wei, H., Li, Q., Zhu, S., Fan, D., & Zheng, Y. (2025). Event-triggered resilient asynchronous estimation of stochastic Markovian jumping CVNs with missing measurements: A co-design control strategy. *Information Sciences, 712*, 122167. [CrossRef]

[12] Li, Q., Zhang, K., Wei, H., Sun, F., & Wang, J. (2025). Non-fragile asynchronous H^{∞} estimation for piecewise-homogeneous Markovian jumping neural networks with partly available transition rates: A dynamic event-triggered scheme. *Neurocomputing*, 130292. [CrossRef]

[13] Pecora, L. M., & Carroll, T. L. (1990). Synchronization in chaotic systems. *Physical Review Letters, 64*(8), 821–824. [CrossRef]

[14] Strogatz, S. H., & Stewart, I. (1993). Coupled oscillators and biological synchronization. *Scientific American, 269*(6), 102–109.

[15] Adiche, S., Larbi, M., Toumi, D., Bouddou, R., Bajaj, M., Belabbes, A., Bouchikhi, N., & Zaitsev, I. (2024). Advanced control strategy for AC microgrids: a hybrid ANN-based adaptive PI controller with droop control and virtual impedance technique. *Scientific Reports, 14*(1), 31057. [CrossRef]

[16] Liu, M., Lu, B., Wang, J., Jiang, H., & Hu, C. (2025). Finite-time and fixed-time synchronization of memristor-based Cohen–Grossberg neural networks via a unified control strategy. *Mathematics, 13*(4), 630. [CrossRef]

[17] Hu, C., Yu, J., & Jiang, H. (2014). Finite-time synchronization of delayed neural networks with Cohen–Grossberg type based on delayed feedback control. *Neurocomputing, 143*, 90–96. [CrossRef]

[18] Cai, Z. W., & Huang, L. H. (2018). Finite-time synchronization by switching state-feedback control for discontinuous Cohen–Grossberg neural networks with mixed delays. *International Journal of Machine Learning and Cybernetics, 9*(10), 1683–1695. [CrossRef]

[19] Chen, C., Li, L., Peng, H., & Yang, Y. (2017). Finite time synchronization of memristor-based Cohen-Grossberg neural networks with mixed delays. *PLoS ONE, 12*(9), e0185007. [CrossRef]

[20] Polyakov, A. (2011). Nonlinear feedback design for fixed-time stabilization of linear control systems. *IEEE Transactions on Automatic Control, 57*(8), 2106–2110. [CrossRef]

[21] Wei, R., Cao, J., & Alsaedi, A. (2018). Fixed-time synchronization of memristive Cohen-Grossberg neural networks with impulsive effects. *International Journal of Control, Automation and Systems, 16*(5), 2214–2224. [CrossRef]

[22] Kong, F., Zhu, Q., Liang, F., & Nieto, J. J. (2019). Robust fixed-time synchronization of discontinuous Cohen–Grossberg neural networks with mixed time delays. *Nonlinear Analysis: Modelling and Control, 24*(4), 603–625. [CrossRef]

[23] Tan, F., Zhou, L., Lu, J., & Zhang, H. (2024). Fixed-time synchronization in multilayer networks with delay Cohen–Grossberg neural subnets via adaptive quantitative control. *Asian Journal of Control, 26*(1), 446–455. [CrossRef]

[24] Liu, A., Yu, W., Huang, L., Guo, J., Lei, T., & Zhao, H. (2023, December). A new method for predefined-time synchronization control of memristive Cohen-Grossberg neural networks. In *2023 IEEE International Conference on Memristive*

Computing and Applications (ICMCA) (pp. 1–6). IEEE. [CrossRef]

[25] Kilbas, A. A. (2006). Theory and applications of fractional differential equations. *North-Holland Mathematics Studies, 204*.

[26] Lundstrom, B. N., Higgs, M. H., Spain, W. J., & Fairhall, A. L. (2008). Fractional differentiation by neocortical pyramidal neurons. *Nature Neuroscience, 11*(11), 1335–1342. [CrossRef]

[27] Zhou, Z. (2025). Stability and synchronization of delayed fractional-order reaction-diffusion Cohen–Grossberg neural networks under perturbation and parameter mismatch. *Asian Journal of Control*. [CrossRef]

[28] Du, F., & Lu, J. G. (2023). Novel methods of finite-time synchronization of fractional-order delayed memristor-based Cohen–Grossberg neural networks. *Nonlinear Dynamics, 111*(20), 18985–19001. [CrossRef]

[29] Zheng, M., Li, L., Peng, H., Xiao, J., Yang, Y., & Zhao, H. (2016). Finite-time stability and synchronization for memristor-based fractional-order Cohen-Grossberg neural network. *The European Physical Journal B, 89*(9), 204. [CrossRef]

[30] Cui, X., Zheng, M., Zhang, Y., Yuan, M., Zhao, H., & Zhang, Y. (2024). Predefined-time synchronization of time-varying delay fractional-order Cohen-Grossberg neural network based on memristor. *Communications in Nonlinear Science and Numerical Simulation, 139*, 108294. [CrossRef]

[31] Assali, E. A. (2021). Predefined-time synchronization of chaotic systems with different dimensions and applications. *Chaos, Solitons & Fractals, 147*, 110988. [CrossRef]

[32] Chen, J., Sun, W., & Zheng, S. (2025). New predefined-time stability theorem and synchronization of fractional-order memristive delayed BAM neural networks. *Communications in Nonlinear Science and Numerical Simulation*, 108850. [CrossRef]

[33] Zhang, S., Yu, Y., & Wang, H. (2015). Mittag-Leffler stability of fractional-order Hopfield neural networks. *Nonlinear Analysis: Hybrid Systems, 16*, 104–121. [CrossRef]

[34] Zhou, J., Li, D., Chen, G., & Wen, S. (2024). Projective synchronization for distinct fractional-order neural networks consist of inconsistent orders via sliding mode control. *Communications in Nonlinear Science and Numerical Simulation, 133*, 107986. [CrossRef]

[35] Kumar, P., & Assali, E. A. (2025). Fixed-time synchronization of fractional-order Hopfield neural networks with proportional delays. *Mathematics and Computers in Simulation*. [CrossRef]

[36] Li, C., & Deng, W. (2007). Remarks on fractional derivatives. *Applied Mathematics and Computation, 187*(2), 777–784. [CrossRef]

Chaouki Aouiti is Professor of Applied Mathematics in the Department of Mathematics, Faculty of sciences of Bizerte at the University of Carthage, Tunisia.

Chaouki Aouiti : graduated from the Faculty of Sciences of Tunis, University Tunis El Manar (1995). He received the M.S. degrees and the Ph.D. in applied mathematics from, National Engineering School of Tunis, University Tunis El Manar, Tunisia, in 1997 and 2003. His Research Area includes artificial neural networks, Computational intelligence, Complex networks, Differential equations, Fractional differential equations, chaotic dynamics, chaos control, synchronization, delay systems, Applied mathematics.

Prof. Aouiti has over 120 publications in peer-reviewed journals and conferences. He has over 3300 citations and an H-Index of 33. He serves as a reviewer of several international journals and a Program Committee for various international conferences.

El Abed Assali is an Assistant Professor in applied mathematics at the University of Jendouba, Higher School of Engineers of Medjez el-Bab (ESIM). He is affiliated with the Laboratory of Geometry, Analysis, and Applied Mathematics (GAMA) - LR21ES10, University of Carthage, Faculty of Sciences of Bizerte (FSB). He received his Ph.D. degree in mathematics from the Faculty of Sciences of Bizerte, University of Carthage, Tunis, in 2020. His research areas include synchronization, chaotic systems, neural networks, nonlinear systems, and time delay systems. (Email: elabed.assali@fsb.rnu.tn)